Emplacement mechanisms of a dyke swarm across the brittle-ductile transition and the geodynamic implications for magma-rich margins

Hans Jørgen Kjøll, Galland Olivier, Loic Labrousse, Torgeir B. Andersen

▶ **To cite this version:**

HAL Id: insu-03188793
https://insu.hal.science/insu-03188793

Submitted on 2 Apr 2021

Emplacement mechanisms of a dyke swarm across the brittle-ductile transition and the geodynamic implications for magma-rich margins

Hans Jørgen Kjøll [a,*], Olivier Galland [b], Loic Labrousse [c], Torgeir B. Andersen [a]

[a] *The Centre for Earth Evolution and Dynamics (CEED), University of Oslo, PO Box 1047 Blindern, NO-0316 Oslo, Norway*
[b] *Physics of Geological Processes, the NJORD Centre, Department of Geosciences, University of Oslo, Norway*
[c] *Sorbonne Université, CNRS-INSU, Institut des Sciences de la Terre Paris, ISTeP UMR 7193, F-75005 Paris, France*

A R T I C L E   I N F O

A B S T R A C T

Igneous dykes are the main magma transport pathways through the Earth's crust, and they are considered to contribute to tectonic extension in volcanic rifts. Dykes are typically considered to result from brittle fracturing, even in the ductile crust. A common assumption is that dyke orientation is controlled by tectonic stresses, such that dykes in rifts are expected to be vertical and perpendicular to extension. Here we report on detailed field observations of a spectacularly well-exposed dyke swarm to show that dykes were not systematically emplaced by purely brittle processes and that dyke orientation may differ from the dominant tectonic stress orientations. The dyke complex formed near the brittle-ductile transition during opening of the Iapetus Ocean and is now exposed in the Scandinavian Caledonides. Distinct dyke morphologies related to different emplacement mechanisms has been recognized: 1) Brittle dykes that exhibit straight contacts with the host rock, sharp tips, en-echelon segments with bridges exhibiting angular fragments; 2) Brittle-ductile dykes that exhibit undulating contacts, rounded tips, ductile folding in the host rock and contemporaneous brittle and ductile features; 3) Ductile "dykes" that exhibit rounded shapes and mingling between the soft ductile host rock and the intruding mafic magma. The brittle dykes exhibit two distinct orientations separated by c. 30° that are mutually cross-cutting, suggesting that the dyke swarm did not consist of only vertical sheets perpendicular to regional extension, as expected in rifts. We were able to use the well-exposed host rock layers as markers to perform a kinematic restoration to quantify the average strain accommodating the emplacement of the dyke complex: it accommodated for >100% extension, but counter-intuitively it also accommodated for 27% crustal thickening. We infer that the magma influx rate was higher than the tectonic stretching rate, implying that magma was emplaced forcefully, as supported by field observations. Finally, our observations suggest that the fast emplacement of the dyke swarm triggered a rapid shallowing of the brittle-ductile transition, and lead to a considerable weakening of the crust. The interpretations presented here could potentially have large implications for surface topography and seismicity in active rifts and volcanic areas around the world.

1. Introduction

Dykes, and igneous sheet intrusions in general, are fundamental magma pathways through the Earth's crust. Their emplacement is controlled by a complex set of factors, such as crustal stress, crustal heterogeneities, topographic loading and magma viscosity (e.g. Spacapan et al., 2017; Kavanagh, 2018; Halls and Fahrig, 1987; Magee et al., 2016). Most models consider dykes as hydrofractures propagating as tensile cracks (mode I) in a brittle fashion with opening perpendicular to the least principal stress, implying

that dykes emplaced in rifts are expected to be vertical and accommodate crustal extension (Keir et al., 2011). Because the rates for dyke emplacement are much higher than the tectonic strain rates, dyke emplacement is assumed to be a brittle process even in the ductile crust (e.g. Rivalta et al., 2015; Sassier et al., 2009; White et al., 2011). The low seismicity in the lower crust in active volcanic rifts, however, questions the purely brittle propagation of dykes in deep crustal levels (e.g. Ágústsdóttir et al., 2016; Legrand et al., 2002; White and McCausland, 2016) and suggest that ductile mechanisms may play a pivotal role in dyke emplacement. In addition, field observations (Spacapan et al., 2017), numerical modelling (Weinberg and Regenauer-Lieb, 2010), laboratory experiments (Bertelsen et al., 2018) and theory (Rubin, 1993)

show that dykes and sheet intrusions can be emplaced by a combination of brittle and ductile deformation of the host rock, namely viscoelastic fingering or ductile fracturing. To what extent ductile deformation accommodates the emplacement of dykes in the ductile crust is still poorly known.

Andersonian theory predicts that the emplacement of dykes is controlled at a first order by far-field crustal stresses (Anderson, 1936; Nakamura, 1977), implying that tectonic stresses dominate over stresses induced by magmatism. Such a scenario is likely when the magma influx rate is lower than the tectonic stretching rate. Field evidence, however, shows that magma influx rates at central volcanoes in rifts can be large enough to produce local magmatic stresses that overcome tectonic stresses, leading to the emplacement of cone sheet swarms (e.g. Burchardt et al., 2013; Pasquare and Tibaldi, 2007). In Large Igneous Provinces, magmatic rates can be extreme at lithospheric scale (e.g. up to 0.78 km^3/yr for the Karoo Basin; Svensen et al., 2012), but the effects of such high influx rate on magma emplacement mechanisms and crustal deformation have not been investigated. Furthermore, the thermal footprint of magmatism related to such major events has been shown to potentially significantly weaken the crust (Daniels et al., 2014; Kjøll et al., 2019). Such weakening strongly depends on the balance between the tectonic stretching rate and the magma influx rate (Daniels et al., 2014). However, geodynamic models of continental breakup associated with Large Igneous Provinces do not account for the thermo-mechanical impact of the magmatism (e.g. Allken et al., 2012). This suggests that the effects of magmatism on the rheological structure of the crust and the tectonic evolution of magma-rich rifted margins need to be addressed and better documented in order to understand the active processes that can be inferred from remote sensing and geophysics, deep within rifts (e.g. Bastow et al., 2011).

In this paper, we report on detailed field observations of a spectacularly exposed dyke swarm emplaced at mid-crustal levels in the magma-rich rifted margin related to a large igneous province that developed during the breakup of the palaeocontinents Baltica and Laurentia, ~605 Ma ago. Our observations allow us to reveal (1) the complex brittle/ductile emplacement of dykes in deep crustal levels, (2) magma emplacement mechanism and related crustal deformation associated with high magma influx rates, and (3) upward migration of the brittle-ductile transition (BDT) because of magmatism.

2. Geological setting

The geological observations presented here are from two distinct regions in northern Norway and Sweden, referred to as Corrovarre and Sarek, respectively (Fig. 1). In Corrovarre, the studied outcrops are from a 0.5 × 6 km lens in a mountainous area. In Sarek, the field area consists of high mountains deeply dissected by glaciers, where high cliffs expose exceptionally well-preserved and large outcrops. Among these we investigated two localities informally named 'Favoritkammen' and 'Favorithelleren' by Svenningsen (1995), using a helicopter to get overview pictures (Fig. 1A and C).

The studied dyke complex can be observed along a string of outcrops spreading 900 km from south to north along the Caledonian mountain belt in Scandinavia (Fig. 1B). The dykes are mostly of basaltic composition and show little chemical variability (Tegner et al., 2019 and references therein). Radiometric dating shows that the dyke complex developed between 616 and 597 Ma (Kjøll et al., 2019 and references therein). Specifically, in Sarek and Corrovarre, new U-Pb dating indicates that the swarms were emplaced at 608 ± 1 and 605.7 ± 1.8 Ma, respectively (Kjøll et al., 2019; Svenningsen, 2001). The dyke complex was part of a magma-rich rifted margin (Abdelmalak et al., 2015; Kjøll et al., 2019) associated with the interaction between a mantle plume (Tegner et al.,

2019) and an active rift system that marked the opening of the Iapetus Ocean (Andréasson et al., 1992, 1998), separating the tectonic plates Baltica and Laurentia (Cawood et al., 2001). The dykes were emplaced in thick packages of Late Neoproterozoic sedimentary rocks (Svenningsen, 1994a). In Sarek, the dykes' host rock consists of evaporitic deposits and carbonates (100-500 m) overlain by a >2500 m-thick succession of arkosic sandstone with thin micaceous layers (Svenningsen, 1994a). At Corrovarre, most of the host rock consist of sandstone, with local discontinuous carbonate layers (Lindahl et al., 2005; Zwaan and van Roermund, 1990). At both Sarek and Corrovarre, geothermobarometry indicate that the dykes crystallized at a pressure of c. 0.3–0.45 GPa, suggesting an emplacement depth of ~10 km (Kjøll et al., 2019), i.e. close to the BDT for a geotherm of 30 °C/km. At Corrovarre, geothermobarometry suggests granulite facies metamorphic conditions at the time of dyke emplacement (Kjøll et al., 2019; Zwaan and van Roermund, 1990), suggesting that the geotherm increased significantly during dyke emplacement.

In the Late Silurian to Early Devonian, the most distal parts of the Baltican margin, which contained the studied dyke complex, was subducted and subsequently exhumed during the Caledonian orogeny (Andréasson et al., 1998). Locally, the dyke complex escaped penetrative Caledonian strain and metamorphism, and remained preserved in large tectonic lenses (Svenningsen, 1994a). The studied outcrops are at the core of these undeformed lenses (Fig. 1). A more comprehensive description of the geological setting can be found in the supplementary material, part 1.

3. Geological observations

Given the large size of the studied outcrops, we performed photogrammetric surveys using an Unmanned Aerial Vehicle (DJI Phantom 4) and pictures taken using a DSLR camera with GPS sensor from a helicopter. The georeferenced images were processed using Adobe Lightroom to enhance contrasts and colours, and subsequently used to compute 3D photogrammetric models, Digital Elevation Models, 3D textured meshes and orthomosaics with the Agisoft PhotoScan Professional software. The 3D mesh generated in PhotoScan was imported in the open source software LIME, developed by the Virtual Outcrop Geology Group, Uni Research CIPR at the University of Bergen, which allows structural measurements of geological planes, by picking three points on the measured surface (Buckley et al., 2017). When outcrops were accessible, direct outcrop observations, measurements and descriptions were conducted.

3.1. Observations in Sarek area

The sedimentary layering of the host rock is sub-vertical, showing large rotation of the exposed crustal block with unknown finite rotations. Nevertheless, the relative orientations of the dykes with respect to each other, and with respect to the sedimentary layering of their host rock, are mostly preserved and primary, given that there is no significant internal tectonic deformation in the studied sub-areas. Cross-bedding, upwards fining sequences and erosional surfaces, all indicate right-way-up toward the south both at the Favoritkammen and Favorithelleren localities (Fig. 2; Svenningsen, 1994b), showing that the current sub-horizontal cross-section represents a vertical profile through the crust. This implies that the Favorithelleren outcrop was deeper than the Favoritkammen outcrop (Fig. 1) since no major shear zone was detected between them. These exceptional exposures allow detailed descriptions of dyke shapes and strain recorded in the host rock in a continuous vertical section for almost 2 km. Structural mapping along the entire profile highlights the presence of brittle, ductile and brittle-ductile structures related to dykes and their emplacement. The following sections report on these respective structures.
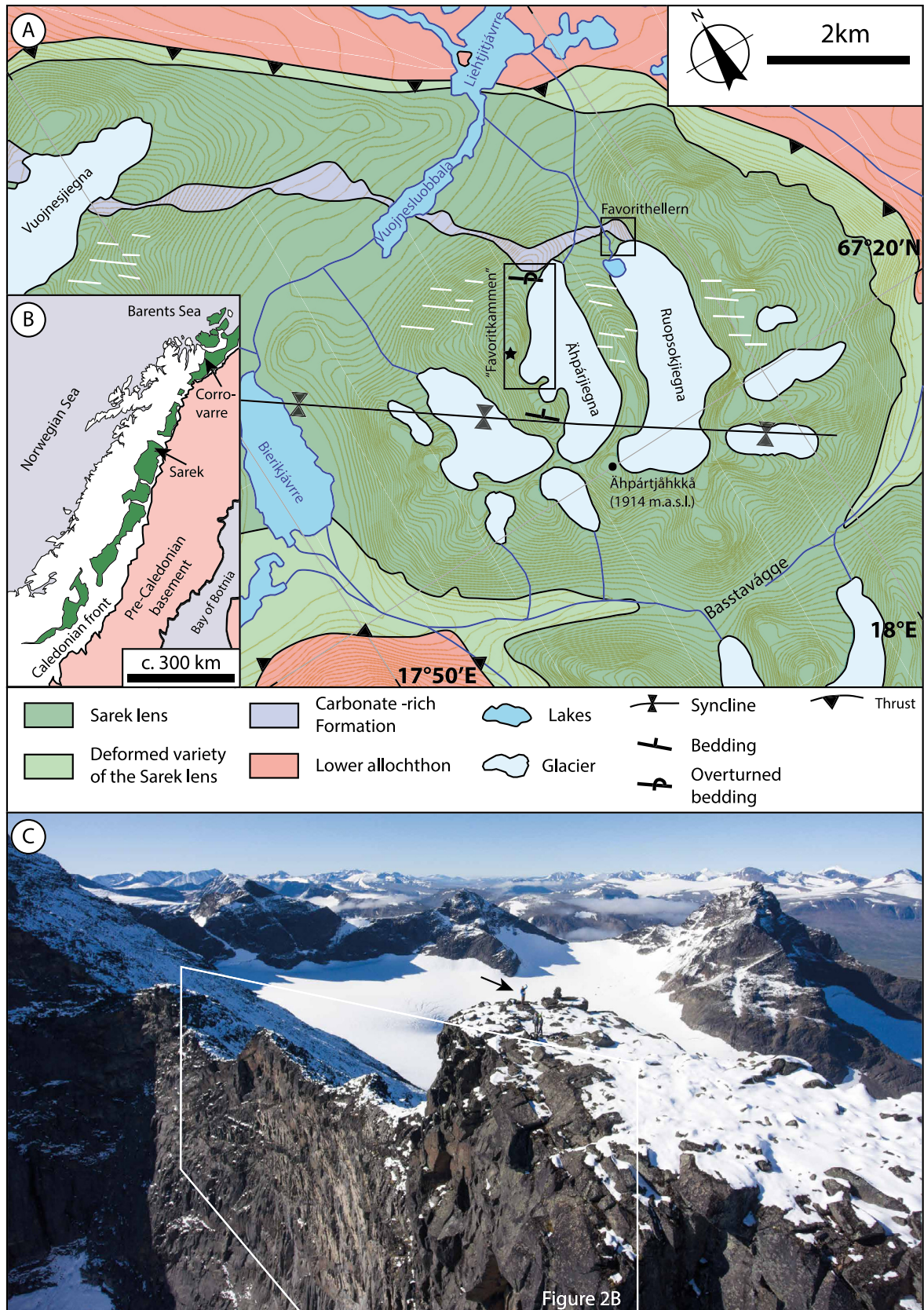
Fig. 1. A) Generalized geological map of Sarek after Svenningsen (1995). Field areas are indicated by black rectangles. Note that bedding is locally overturned on the north limb of the syncline. White lines indicate orientation of dykes. Black star indicates location of the geologists in Fig. 1C. B) Simplified geological map of the central and northern Scandes. White (and green) areas are rocks affected by Caledonian deformation. Green areas indicate the extent of the variably metamorphosed pre-Caledonian margin of Baltica. Pink is basement unaffected by Caledonian deformation and metamorphism. C. Photograph of the summit of the Favoritkammen cliff (geologists for scale highlighted by arrow), in Sarek. The only access was with a helicopter. This picture shows the remoteness and inaccessibility of many of the key field localities in Sarek National Park, north of the polar circle in Sweden. (For interpretation of the colours in the figure(s), the reader is referred to the web version of this article.)
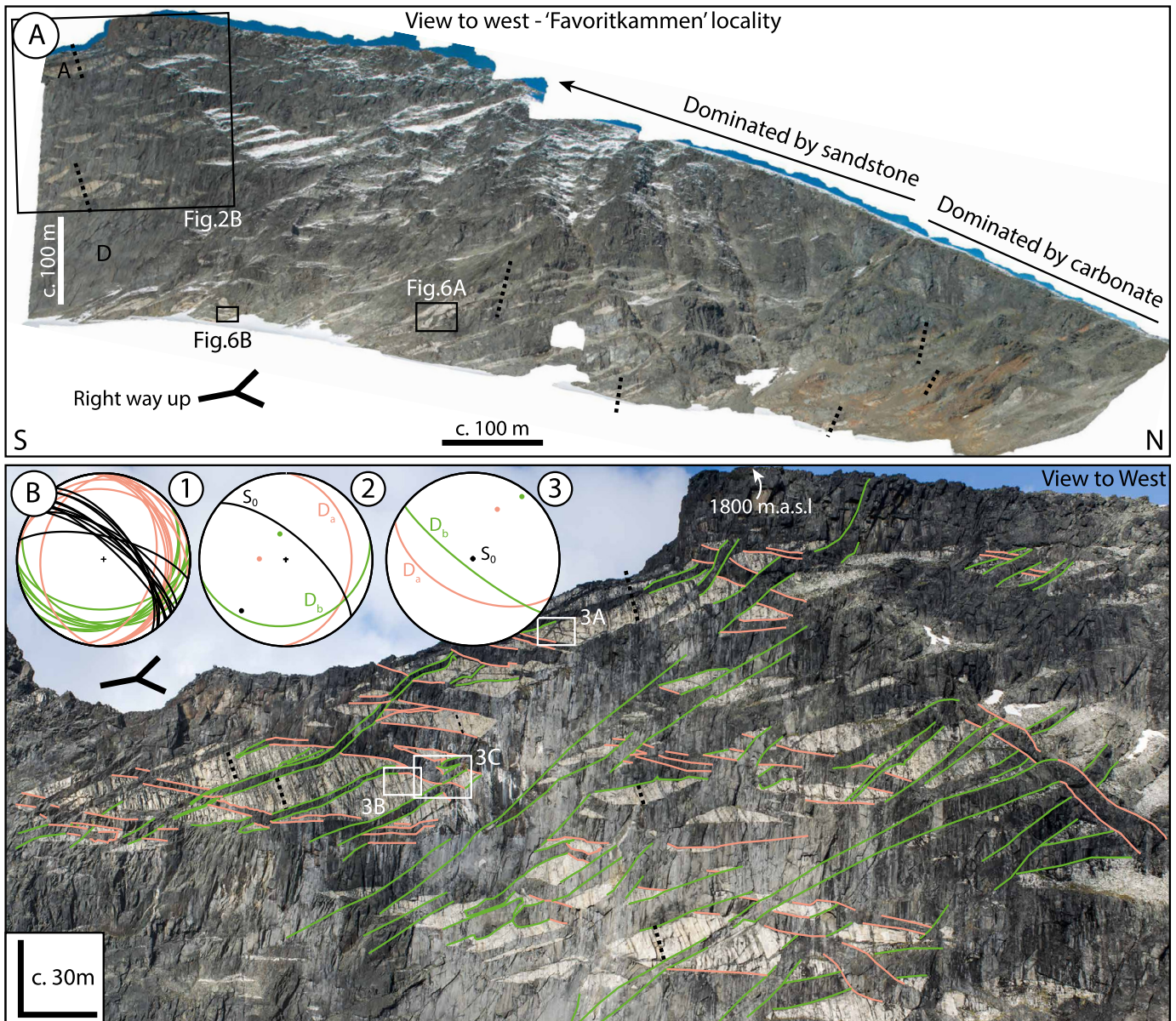
Fig. 2. Overview photographs of the "Favoritkammen" locality, a 200 m tall, vertical cliff wall in Sarek National park, northern Sweden. Sedimentary layering is indicated by black dashed lines. A) Overview of the entire "Favoritkammen", c. 1.5 km long, continuous outcrop that show both brittle, ductile and brittle-ductile structures related to the dyke emplacement. Some topography causes some distortion of the composite orthomosaic. Black rectangles show location of respective figures. D: Dolerite, A: Arkose. B) Detailed composite photograph of a small part of Favoritkammen, where dykes are colour coded according to orientation. Note that the dykes with the different orientations are mutually cross-cutting i.e. D_a (orange) cuts D_b (green) and vice versa. In addition, at several localities the dykes bend and change direction (e.g. Fig. 3A and D). Stereonet #1 shows raw data acquired from 3D outcrop model. Note that the dykes form two groups, one E-dipping and one SSE-dipping. Stereonet #2 shows the present average dyke orientation for the two dyke groups and the bedding, denoted D_a, D_b and S_0, respectively. Stereonet #3 shows average dyke orientations for the two dyke groups when bedding is rotated to horizontal. Where cross-cutting relationships can be discerned they are colour coded according to the stereonets.

3.1.1. Brittle structures

The dykes at the Favoritkammen cliff appear as relatively straight segments (Fig. 2 and Fig. 3). The contacts are very sharp and regular. Locally, gentle undulations of the contacts are visible (Fig. 3A). Only a few dyke tips have been identified in the area. They appear as very sharp tips terminating wedge-shaped dykes that are significantly thinner than the other dykes (Fig. 3C). These thinner dykes also exhibit regular and straight contacts with the host rock. Local jogs/deflections are common along the strike of the dykes where the dykes cross-cut thin micaceous layers between quartzite beds (Fig. 3C, inset). It is noticeable that even if the host rock is strongly layered, no sill, i.e. layer-parallel intrusion, is observed. Where dyke segments are arranged in en-echelon pattern, bridges develop between segments. Generally, these bridges

are broken with irregularly shaped pieces of host rock floating in the dyke where it steps (Fig. 3D).

Outcrop-scale observations at Favorithelleren show that most dykes exhibit chilled margins (Fig. 3B. When both dyke walls are in contact with the sedimentary host rock, dykes display double-sided chilled margins. Stacked dykes and sheeted dykes (Fig. 2 and Fig. 3), with a more complex chilled margin distribution, have also been observed.

The complete exposure at Favoritkammen and Favorithelleren allowed a reconstruction of the entire outcrop on virtual 3D models, which were used for systematic measurements of 212 dyke thicknesses as well as the orientation of some of the dykes and the strike/dip of the bedding in the host rock (Fig. 2 and Fig. 3). Note that the dyke thicknesses are measured on the 3D models,
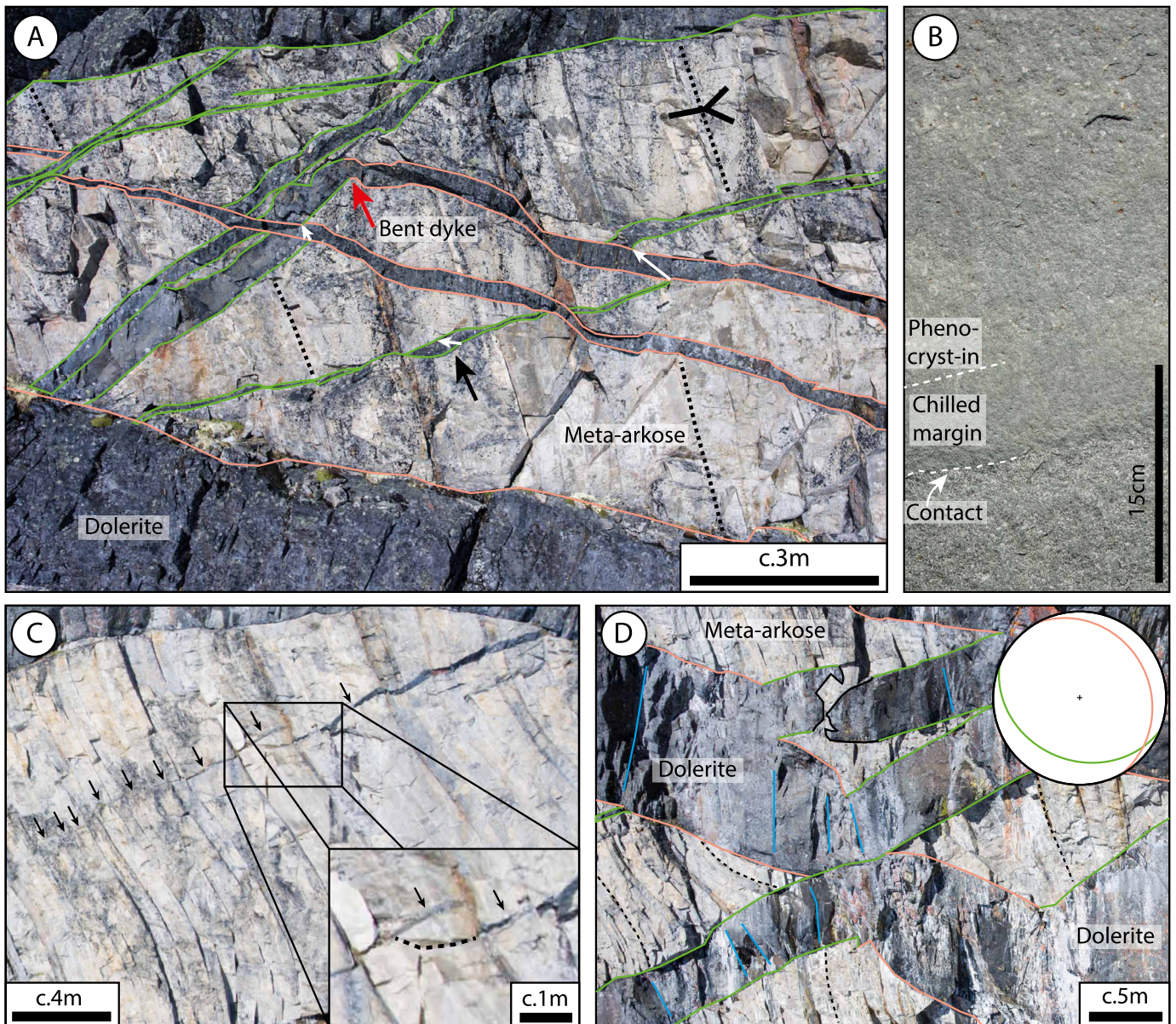
Fig. 3. Overview figure of areas where the dyke emplacement primarily is controlled by brittle mechanisms. A) Complex cross-cutting relationships between the two orientations of dykes displayed in Fig. 2a. The central dyke, highlighted with a red arrow, displays a dramatic bend of c. 80° from D_a to D_b. Black arrow indicates transtensional opening of a dyke. Opening vectors are drawn as white arrows. The opening is constrained to the sandstone layers with minimal opening in the argillaceous domains between the pure sandstone layers. Black dashed lines indicate bedding in meta-arkose. B) Chilled margin at contact between two dykes. White dashed line indicates chilled margin. C) Thin, dyke tip propagated orthogonal to bedding. Somewhat affected by heterogeneities in the host rock as seen in the insert. Here the dyke made an abrupt shift in direction at the end of the sandstone bed, but the fracture propagated straight before bending in (dashed line in zoom) D) Two dykes with sharp and dramatic bends. Orientation is measured directly in 3D model and plotted in stereonet. Joints, orthogonal to the dyke margin can be observed in both dykes marked by blue lines. Black dashed lines indicate bedding in meta-arkose. Note partially broken bridge with angular edges.

such that they are estimates of the true thicknesses, not the apparent thickness on the cliff. The measurement was taken away from tips and where the dyke segments were assumed to display an average thickness. The measured dyke thicknesses range from 0.2 m to 18 m, the mean value being 5.2 m and the median being 4.5 m (Fig. 4). Fig. 4 displays the histogram of the dyke thickness, which exhibits a significantly right-skewed distribution. Following Krumbholz et al. (2014), we fitted our dataset with a Weibull probability function, the fitting parameters being listed in Fig. 4. Note that all measured dykes presented here intrude arkose and not the underlying carbonate, meaning that the thickness distribution is not affected by distinct host rock lithologies.

The spectacular outcrop at Favoritkammen shows that the dykes are not all parallel. The methodical measurements of the dyke orientations show two dominant trends, one dipping to the ENE (orientation D_a, orange on Fig. 2 and Fig. 3) and one dipping to the south (orientation D_b, green on Fig. 2 and Fig. 3). These two main orientations are separated by an average acute angle of ca. 30°. D_a is sub-orthogonal to bedding (83° precisely) while D_b shows an acute angle of 53° (Fig. 2A). We observe mutual cross-cutting relation between the D_a and D_b dyke populations, meaning that the two populations are contemporaneous (Fig. 2 and Fig. 3A). In addition, we locally observe sharp bends between long dyke segments of distinct orientations, highlighting that a single dyke can have segments with orientation D_a and other segments with orientation D_b (Fig. 2 and Fig. 3A and D).
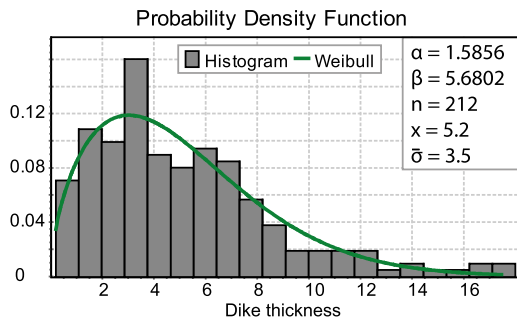
Fig. 4. The probability density function of the dykes follows a Weibull distribution. α is the shape parameter and β is the scale parameter of the distribution. n denotes the number of measured dykes. $\bar{x}$ and σ denote the mean and standard deviation, respectively. Measurements have been done directly on the 3D model where the exposed dyke segment appears to display an average thickness.

On the cliff of Favoritkammen, the host rock of the dykes is remarkably well exposed and well preserved from the Caledonian deformation and regional metamorphism. The sedimentary layering is visible throughout, forming massive beds that range in thickness from a few tens of centimetres to several metres (Fig. 2 and Fig. 3). Remarkably, the sedimentary layers exhibit very little deformation, except gentle bending (Fig. 3C and D). We correlated the layer sequences on both sides of the dykes by utilizing characteristic markers in the meta-sediments, such that it was possible to reconstruct the kinematics associated with the emplacement of each dyke. Such reconstruction shows that the mode of opening of most dykes is oblique to the dyke walls, implying mixed mode I and mode II fracturing (Fig. 3A). Furthermore, this leads to an apparent offset of early dykes cross-cut by later dykes (Fig. 3A).

Based on these observations, we performed a 2D strain restoration of the Favoritkammen outcrop, in order to quantify the strain induced by the emplacement of the dyke complex (Fig. 5). The restoration method is described in supplementary material, part 2. The calculated strain ellipse deduced from eigenvectors of the 2D strain field tensor indicates that the intrusion of the dykes is responsible for an overall 2D dilatancy of 147%, which is consistent with volume addition due to magma injection (Fig. 5). However, this measured dilatancy is not isotropic, as illustrated by the non-equidimensional calculated strain ellipse (Fig. 5): the maximum stretching (X_{max}) is 194%, while the minimum stretching (X_{min}) is 127%. We observe that the axis of maximum stretching is sub-perpendicular to the direction of the dyke family D_b, and oblique to the direction of the dyke family D_a. We note as well that the maximum stretching direction is oblique to the bedding.

3.1.2. Brittle-ductile structures

At the base of the Favoritkammen cliff (Fig. 1A and 2B), the shapes and structures of the dykes are different than those observed in the upper parts of the cliff (Fig. 2B). Contacts between the dolerite and the host rock are still sharp, but they are not planar, and they often display wavy boundaries and complex morphologies such as pinch-and-swell structures (Fig. 6A). The intrusions also exhibit significant thickness variations (Fig. 6A). The host rock layers appear much more deformed (Fig. 6A). The outcrop of Fig. 6B provides very precise relationships between successive dykes and the host rock. There, an early large dyke was emplaced (Dolerite #1 in Fig. 6B), with a thin wedge-shaped offshoot sheet characteristic of brittle fracturing (highlighted by white arrows in Fig. 6B). The thin offshoot is cross-cut by a later thicker dyke (Dolerite #2 in Fig. 6B), which has an en-echelon configuration with two branches, separated by a broken bridge with both sharp angular and rounded contacts with the host rock. The host rock layering as well as the thin offshoot from dolerite #1, below the lower branch of dolerite #2 is planar, whereas the thin offshoot dyke
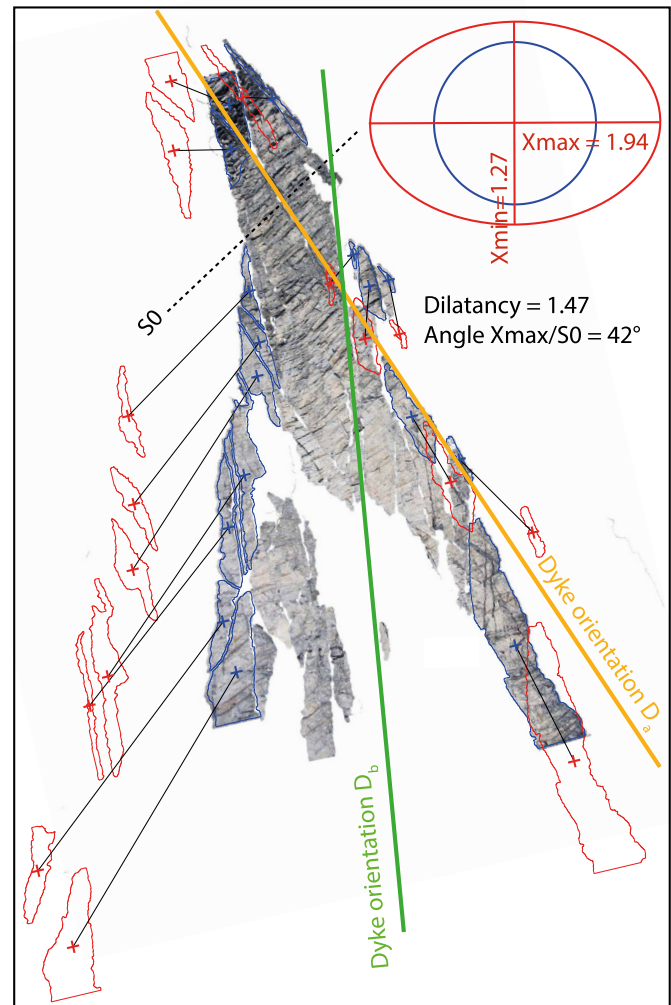

Fig. 5. Diagram showing estimates of inverse strain ellipse related to dyke emplacement in two dimensions. Pre-intrusion geometry was reconstructed by correlating host-rock markers in the orthorectified image of Fig. 3A. These markers were used to restore back the host-rock polygon centroids to estimate homogeneous strain ellipse. This method does not account for any out of plane motion.

above dolerite #2, as well as the host rock layering, are folded. Note that the outcrops of Fig. 6A and B are at a very similar stratigraphic level as those of Fig. 3 (see locations in Fig. 2), with the same host rock lithology (arkosic sandstone).

Outcrop observations at the Favorithelleren locality shows that the carbonate layers of the host rock exhibit folds near a dyke, with axial plane parallel to the dyke contact (Fig. 6C). Centimetre-scale reverse shear zones affect calc-silicate layers of the host rock a few centimetres away from the dyke wall. Both folds and reverse shear zones accommodate ductile and brittle shortening perpendicular to the dyke wall. Fig. 6D displays another intrusive contact at Favorithelleren, which displays a very irregular, "blobby" shape showing local melting of the host rock. The sedimentary layering is bended at the intrusion contact. Note that the outcrop of Fig. 6D is located in a higher stratigraphic position than the outcrop of Fig. 6C.

3.2. Observations from the Corrovarre lens

The topography at Corrovarre is much smoother and lower than at Sarek, such that the studied outcrops are discontinuous because of vegetation and local slope deposits. Detailed outcrop observations highlight the presence of brittle-ductile and ductile structures
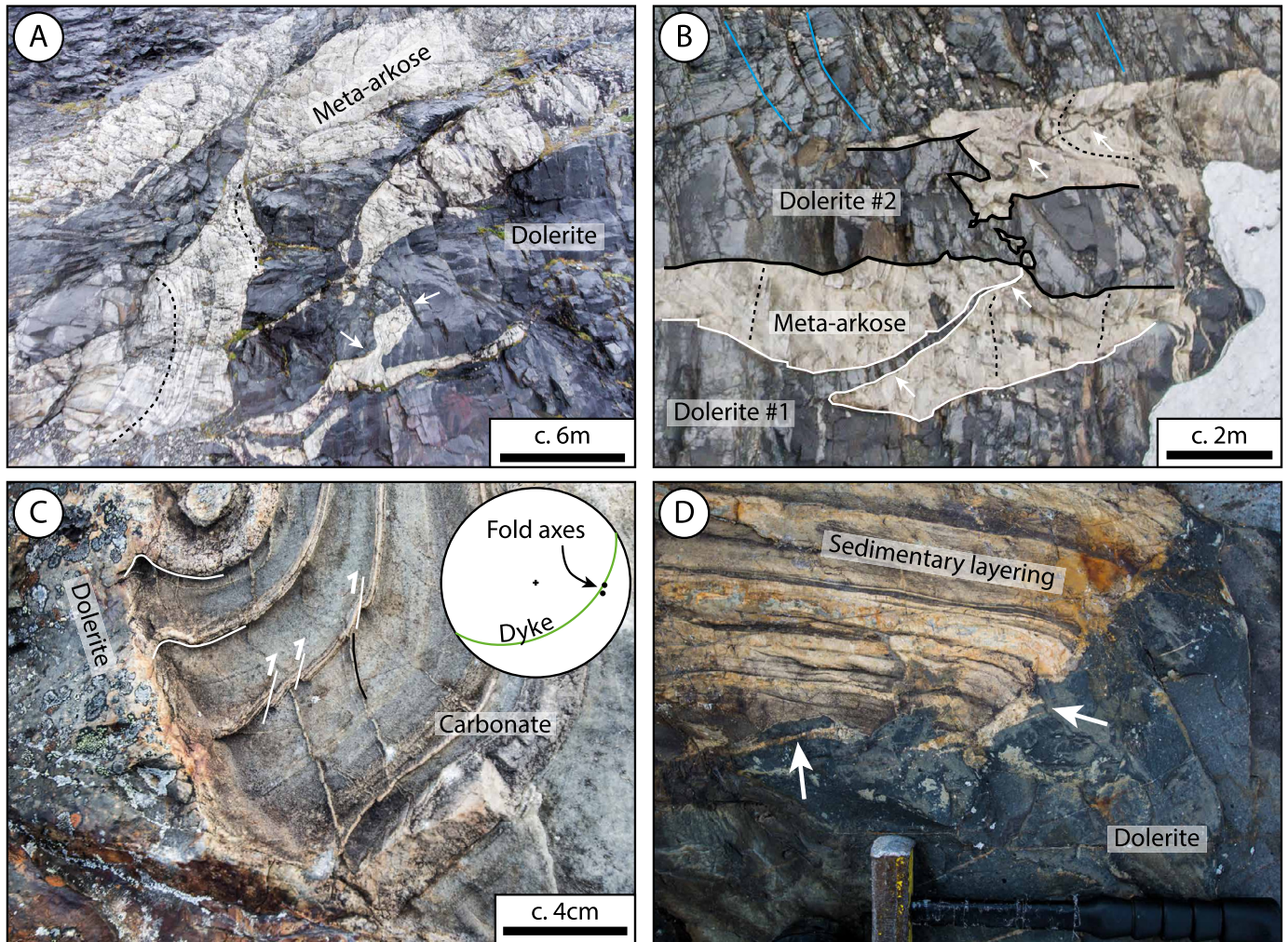
Fig. 6. Overview plate showing evidence for brittle-ductile deformation related to the emplacement of mafic dykes in Sarek. A) Complex geometric relations between dykes and bridges in the Favoritkammen locality. Dashed black lines indicate bedding in the arkose. White arrow points to rounded bridge in the host rock. B) Shows the temporal evolution of the BDT as dolerite #1 shows a thin, tapered dyke offshoot which intruded meta-arkose, highlighted by white line and arrows. This thin offshoot is subsequently folded as dolerite #2 is emplaced. Black dashed line indicate bedding in the meta-arkose. Blue lines indicate preserved columnar jointing in a later dyke. C) Carbonate with stronger calc-silicate layers show small scale thrust faults duplicating the calc-silicate layers as well as folds with axial planes parallel to dyke contact. D) Leucosomes (white arrows) forming at the contact between a sedimentary rock and a dolerite.

related to the dykes and their emplacement. Purely brittle structures have not been observed.

3.2.1. Brittle-ductile structures

A cliff in the southern part of the Corrovarre lens displays several mafic dykes emplaced in similar arkosic sandstone as those of the Favoritkammen outcrop described above (Fig. 7A). The intrusive contacts are sharp. Some contacts are relatively straight, whilst others exhibit more irregular curved shapes. A few dyke tips are visible at the outcrop, and they are all blunt and rounded, which is markedly different from the dyke tips observed in Sarek. The sedimentary layers are draped around the dyke tip and cut by a swarm of fractures that radiate from the tip of the dyke (Fig. 7B), showing that the host rock behaved in a brittle and ductile manner in response to the imposed stress associated with the propagating dyke tip.

3.2.2. Ductile structures

Throughout Corrovarre, we found numerous outcrops of mafic intrusions exhibiting highly irregular shapes. Fig. 8A displays a string of dolerite pillows within a migmatitic arkose, where migmatization is regional, but there is no evidence for Caledonian deformation. Extensional Crenulation Cleavage (Fig. 8B) struc-

tures within the migmatites are cross-cut by the dyke swarm, implying that regional shearing and stretching was accommodated prior to intrusion. We also found other irregular doleritic intrusions emplaced within marbles. Fig. 8C displays a lens-shape dolerite draped by the foliation in the marble, resembling a tectonic boudin. The dolerite-marble contact is sharp, with local angular apophyses. The dolerite exhibits a chilled margin at the contact, the magmatic texture is preserved, and it does not display any evidence of tectonic deformation. The dolerite also has regular columnar jointing perpendicular to the lens contacts (blue lines in Fig. 8C). The right tip of this dolerite body is highly irregular, with complex lobes resembling mingling structures that are in angular contact with the foliation of the host marble (Fig. 8D). All these observations evidence that the shape of the dolerite body is primary, i.e. of intrusive origin.

4. Interpretation

4.1. Emplacement mechanisms of individual intrusions

Most of the dyke segments in Sarek exhibit regular and straight contacts with the host rock and sharp and thin tips (Fig. 3A and D). The thin dykes exhibit a clear wedge shape. In addition, angular
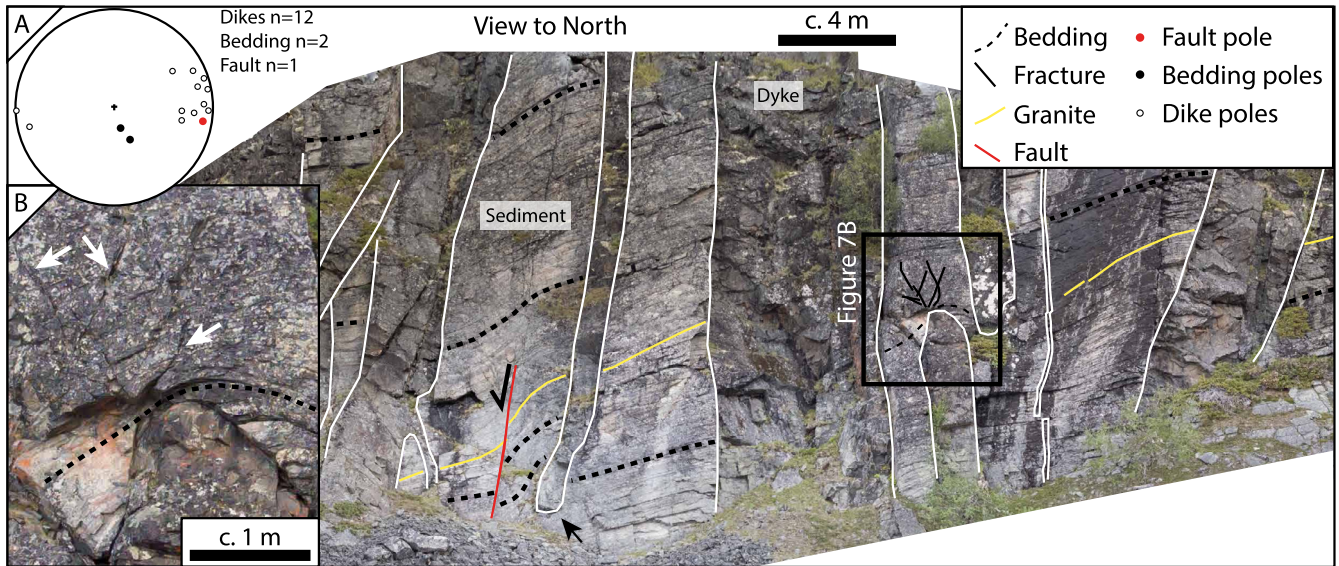
Fig. 7. Figure showing details from a cliff in southern Corrovarre. A) Overview of the cliff. Stereonet shows structural data of the dykes and host rock. White lines outline dykes. Note a granitic vein, cut by mafic dykes. Note also the shape of the dykes, which exhibit equal thickness of the dykes, which abruptly terminate in a blunt tip. B) Detail of a dyke tip shows bedding wraps the tip and fractures cutting the folded bedding ahead of the tip (white arrows).
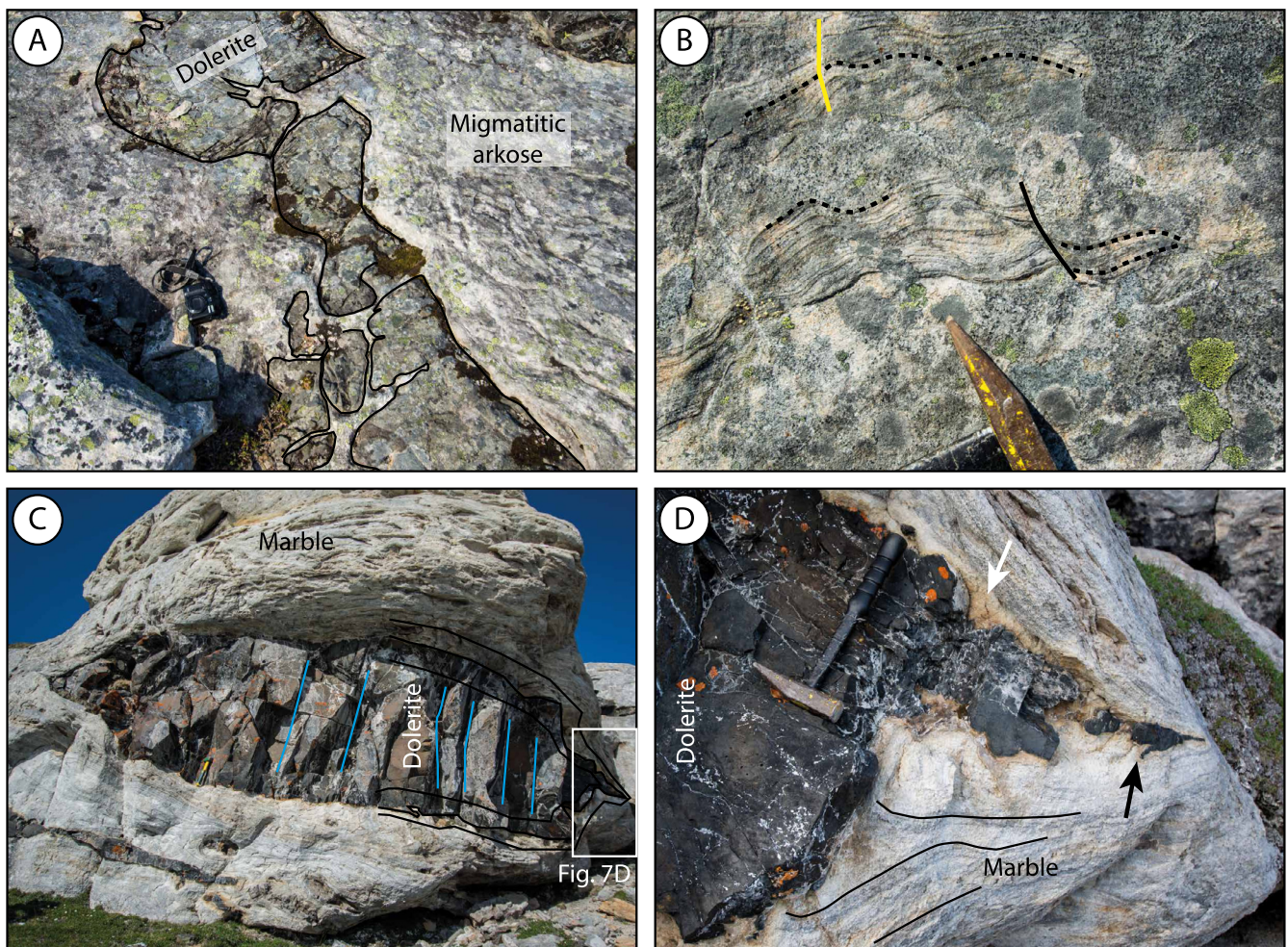
Fig. 8. Overview plate of the northern segment. A) Mafic magma which intruded a soft migmatitic arkosic sandstone formed tortuous contacts and complex lobes. Digital camera for scale B) ECC fabric in the migmatitic arkose shows layer-parallel stretching and intrusion local leucosomes (yellow line). C) Dolerite magmatic "boudin" in marble. Dolerite shows cooling joints (blue lines), c. 10-15 cm thick chilled margin, and a contact metamorphic aureole seen as a discolouration of the marble at the contact between dyke and marble. Note hammer for scale in the central left of the image. White rectangle shows location of picture but note that the photograph in D is taken at a different angle than C. D) Magmatic "boudin" neck. White arrow indicates contact metamorphic aureole as a yellow-ish discolouration. Black arrow shows the complex lobes at the "boudin" neck, resembling Saffman-Taylor structures (Saffman and Taylor, 1958), suggesting a magmatic origin. Note that the dolerite cut the foliation in the marble.

broken bridges separate dyke segments, where angular clasts of the host rock are often observed surrounded by crystallised mafic dyke (Fig. 3C). From these observations we infer that the emplacement of most of the dykes was primarily controlled by brittle fracturing of the host rock, in good agreement with established models of dyke emplacement (e.g. Rivalta et al., 2015). This conclusion is corroborated by the measured Weibull distribution of the dyke thicknesses, in agreement with the field measurements of Krumbholz et al. (2014), who interpreted such a thickness distribution by brittle failure of the crust with distributed weaknesses of different sizes.

Conversely, other dykes exhibit distinct shapes and associated structures related to other emplacement mechanisms. The intrusions of Fig. 6A and B at Favoritkammen exhibit irregular and wavy contacts, and their host rock exhibit significant ductile folding. In addition, observed broken bridges along these intrusions exhibit highly irregular, rounded shapes (Fig. 6A and B). The detailed observations at Favorithelleren (Fig. 6C) highlight coeval ductile folding and brittle faulting of the host rock layers near a dyke wall. Finally, the dyke of Fig. 7 at Corrovarre exhibits parallel walls and a blunt tip, and both ductile doming and brittle fracturing of the host rock ahead of the tip. It is important to note that the observed ductile deformation is not related to Caledonian regional tectonics, as (1) the brittle/ductile features of Fig. 6C and Fig. 7B are restricted to the vicinity of the intrusions, and (2) the ductile deformation visible in Fig. 6B only affects the early dykes but not the later ones. We infer from these observations that these intrusions were emplaced by viscoelastic fracturing or viscoelastic fingering (Bertelsen et al., 2018).

The local brittle/ductile deformation on Fig. 6C is related to shortening perpendicular to the dyke wall. In addition, the ductile bending, and associated fracturing, ahead of the tip of the dyke on Fig. 7B suggest that the dyke tip was pushing its host rock ahead. These observations show that the emplacement of the magma in the ductile-brittle crust is a forceful process, such that the overpressured magma deforms its host rock to create its own space, even in a rifting setting. To accommodate the increasing magma volume, the host rock deforms either by brittle failure, ductile flow, or both at the same time.

Numerous intrusions in the Corrovarre area exhibit complex shapes, such as lenses (Fig. 8) and pillow-like shape (Fig. 8A). In addition, the host rock exhibits significant ductile foliation draping around the intrusions. These structures could casually be interpreted as post-emplacement tectonic boudins, however, chilled margins observed at the contacts of the igneous bodies show that they are primary emplacement features. The close-up photographs of Fig. 8A and D show that the intrusion contacts are highly irregular with complex lobes. Note that on Fig. 8A, the host rock was partially molten when the dolerite was emplaced. Such morphology strongly resembles a Saffman-Taylor instability (Saffman and Taylor, 1958), which develops during the inflow of a viscous fluid into another fluid of higher viscosity. These structures are also very similar to intrusions emplaced in low-viscosity salt diapirs (Schofield et al., 2014). These observations show that the emplacement of these intrusions was dominantly controlled by ductile deformation of the host rock, which behaved as a relatively low viscosity fluid.

Our observations at Sarek show that magma emplacement was dominantly accommodated by brittle deformation and mixed ductile/brittle deformation in the meta-arkose sandstone and the slightly deeper carbonates, respectively (compare Fig. 3 and Fig. 6C). Locally, Fig. 6C shows that ductile folding affects carbonate layers, whereas brittle faulting offset calc-silicate layers. Finally, our observations at Corrovarre show that magma emplacement was dominantly accommodated by mixed ductile/brittle to entirely ductile deformation in the meta-arkoses and the carbonate sediments, respectively (compare Fig. 7 with Fig. 8). Such systematic differences show how the host rock and their associated rheologies are critical factors controlling magma emplacement and the morphologies of the intrusive bodies.

4.2. Emplacement of the whole dyke swarm

The Favoritkammen outcrop allows the identification of two groups of dykes with distinct orientations, separated by an acute angle of ca. 30°. Their mutual cross-cutting relationships, and the sudden shift from one direction to another along a single dyke (Fig. 2 and Fig. 3) show that these two dyke groups were contemporaneous and not the result from two successive intrusive episodes. This implies that the studied dyke swarm is not a simple stack of parallel dykes perpendicular to the least principal stress (here extensional stresses related to rifting), as expected from the Anderson's theory (Anderson, 1905). We therefore infer that many of the studied dykes were not vertical at the time of emplacement but had a dip of 70° or less.

The restoration shown in Fig. 5 displays that the dyke swarm accommodated for large crustal stretching (94%), as expected in rifts. However, counter-intuitively, the restoration also indicates that the positive dilation associated with the dyke swarm also accommodated for 27% of crustal thickening (Fig. 5). This shows that the emplacement of a dyke swarm also can contribute to significant crustal thickening, even in a rift setting. Such a mechanism is only possible if the emplacement of the dyke swarm is a forceful process, as corroborated by local-scale structural observations (see section 4.1). We infer that the magma influx rate was larger than the tectonic stretching rate, such that the tectonic extension was not fast enough to accommodate for the input of magma. This is corroborated by high-precision radiometric (U-Pb zircon) dating of the dykes, which suggests that the whole dyke swarm was emplaced in a period of ∼4 Ma or less (Kjøll et al., 2019), which is significantly shorter than characteristic time scale of continental rifting (e.g. Courtillot et al., 1999; Menzies et al., 2002).

In both the Sarek and Corrovarre areas, we observed brittle as well as ductile deformation accommodating the emplacement of the studied intrusions. Based on this study and the previous estimates of pressure-temperature conditions for the magma emplacement (650–700 °C and 3-4 kb from the contact metamorphic aureole; Kjøll et al., 2019), we infer that the studied intrusive complex was initially emplaced near the BDT. In addition, Fig. 6B shows that an early thin, sharp-tipped dyke, the emplacement of which was likely controlled by brittle deformation, has been folded in ductile fashion to accommodate the emplacement of later dykes. This suggests that earlier dykes were emplaced in a brittle crust, whereas later dykes at the same stratigraphic level were emplaced in a more ductile crust. This strongly suggests that the BDT moved upward with time during the emplacement of the dyke swarm. Such an upward migration of the BDT is likely a response to the heating of the crust resulting from the fast influx of mafic magma (Daniels et al., 2014).

5. Discussion

5.1. Regional constraints

In this study, we integrate field observations from two localities, Sarek and Corrovarre, which are separated by ∼300 km in the Seve and Kalak nappe complexes of the Caledonides and has been transported over large distances (e.g. Jakob et al., 2019). The similarities in exposed crustal depth, in intrusion age and host rock lithologies strongly suggest that these areas can be correlated, and that the studied intrusions represent the same magmatic event. The
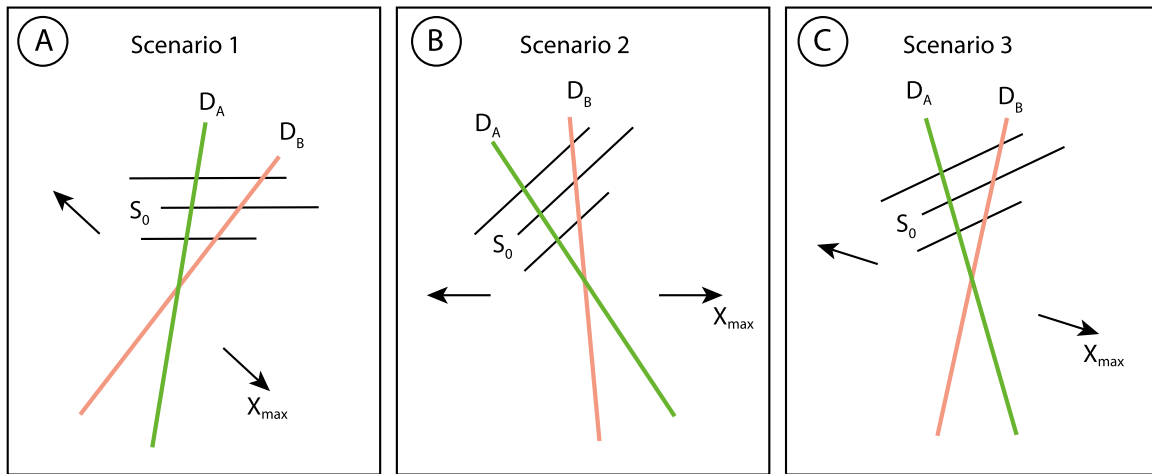
Fig. 9. Configuration of dykes (D_A and D_B), bedding (S_0) and direction of maximal stretching (X_{max}). Three indistinguishable scenarios are proposed. Note that all three scenarios result in at least one dyke orientation being inclined. A) Bedding was horizontal at time of emplacement. B) The maximum stretching direction was horizontal at the time of emplacement. C) The bisector line of the obtuse angle between the two dyke sets marks the horizontal.

Caledonian deformation rotated the crustal block exposed at Sarek, such that it is challenging to reconstruct the palaeo-horizontal at the time of emplacement of the dykes. Our observations, however, allow us to propose three scenarios to discuss the palaeo-horizontal at the time of dyke emplacement (Fig. 9). In scenario 1, the host rock layering S_0 is sub-horizontal and the dykes with orientation D_a are sub-vertical (Fig. 9A). In this case, the dykes with orientation D_b and the finite maximal stretching direction calculated in Fig. 5 are inclined. We would interpret the inclined finite maximal stretching direction, as a result of a syn-intrusion tectonic shear. In scenario 2, the main stretching direction of Fig. 5 is horizontal, and the dykes with orientation D_b are sub-vertical (Fig. 9B). In this case, the host rock layering is already tilted and the dykes with orientation D_a are inclined. Finally, in scenario 3, the two dyke orientations are a conjugate fracture set related to syn-magma emplacement, and the bisector line of the obtuse angle marks the palaeo-horizontal (Fig. 9C). In this case, the host rock layering is tilted and both dyke orientations D_a and D_b are inclined. Our observations do not allow us to distinguish between these three scenarios. Nevertheless, in all three cases, at least one dyke orientation is inclined, and we interpret that the opening of these dykes accommodated for the observed crustal thickening. Hence these three scenarios are compatible with crustal thickening induced by the emplacement of the dyke swarm.

### 5.2. Tectonic and geodynamic implications for magma-rich margins

The geodynamic interpretation of crustal thickening resulting from the emplacement of the dyke swarm strongly relies on the robustness of the kinematic restoration of Fig. 5. This kinematic restoration was computed from a 2D cliff section, whereas the restored objects are 3D. The dykes are, however, almost perpendicular to the cliff, and so the exposed outcrop is very close to display the section perpendicular to the dyke segments and therefore we infer that the kinematic restoration in the plane of the cliff is reliable. We cannot rule out some out-of-plane displacements, which are not reachable with our method. However, the geodynamic setting at the time of dyke emplacement was inferred to have a limited, if not negligible, trans-tensional component implying that out-of-plane kinematics is likely limited (Svenningsen, 1995).

The emplacement of the studied dyke swarm accommodates for almost 100% stretching (β-factor = 1.94; Fig. 5), as expected in a rift setting. However, more surprisingly the restoration indicates that the emplacement of the dyke swarm accommodated

27% of crustal thickening. Such thickening was possible because the dyke swarm consisted of at least one dyke population that was not vertical and not oriented perpendicular to the rifting direction (Fig. 9). Furthermore, we show that some dyke segments are emplaced as mixed mode I and II, which increases the amount of thickening relative to an inclined dyke opening as a mode I fracture (Fig. 3A). Their opening vector therefore had a vertical component resulting in crustal thickening. We infer that the tectonic stretching rate did not balance the rate of magma injected in the crust, hence the magma input dominated over the tectonic extension. This is supported by the high-precision radiometric dating, which shows that the peak magmatic event occurred within a short period of time (∼4 Ma; Kjøll et al., 2019) and is in good agreement with estimated short durations of magmatism related to Large Igneous Provinces (e.g. Svensen et al., 2012; Tegner et al., 2019). The observations presented here suggest that voluminous and fast emplacement of large dyke swarms at depths of 10 to 14 km can contribute to significant crustal thickening, even in rifting settings, if the magma influx rate is larger than the tectonic stretching rate. Our observations differ from common observations in "normal" volcanic rifts and rift zones of hot spot volcanism, where dyke emplacement is often accompanied by normal faulting (e.g. Rubin, 1992). In these settings, magma influx rates are significantly lower than those in LIPs, and we suggest that the magma influx rate did not fully balance the tectonic stretching rate.

The thickening accommodated by the emplacement of the dyke swarm is estimated to ∼27% (Fig. 5). If this thickening is applied to a normal 15-km thick brittle crust, this can lead to ∼4 km of crustal thickening. Unless accommodated for by dyke induced normal faults in the upper crust, such thickening would result in substantial surface uplift (Fig. 10). In Large Igneous Provinces, uplift is observed and systematically interpreted as dynamic topography resulting from the interactions between a rising viscous plume and the overlying lithosphere (e.g. Pik et al., 2008). Our observations suggest instead that at least parts of this uplift may be caused by the emplacement of a dyke swarm in the crust. Such thickening can explain the presence of thick distal crustal segments (so-called outer highs) along magma-rich margins (e.g. Mjelde et al., 2001). This is supported by recent geophysical observations that an outer high in the mid-Norwegian margin likely hosts a dense dyke swarm (Abdelmalak et al., 2015).

The field observations from Sarek suggest that the BDT may have moved upward during the ∼4 Ma-long period of emplace-
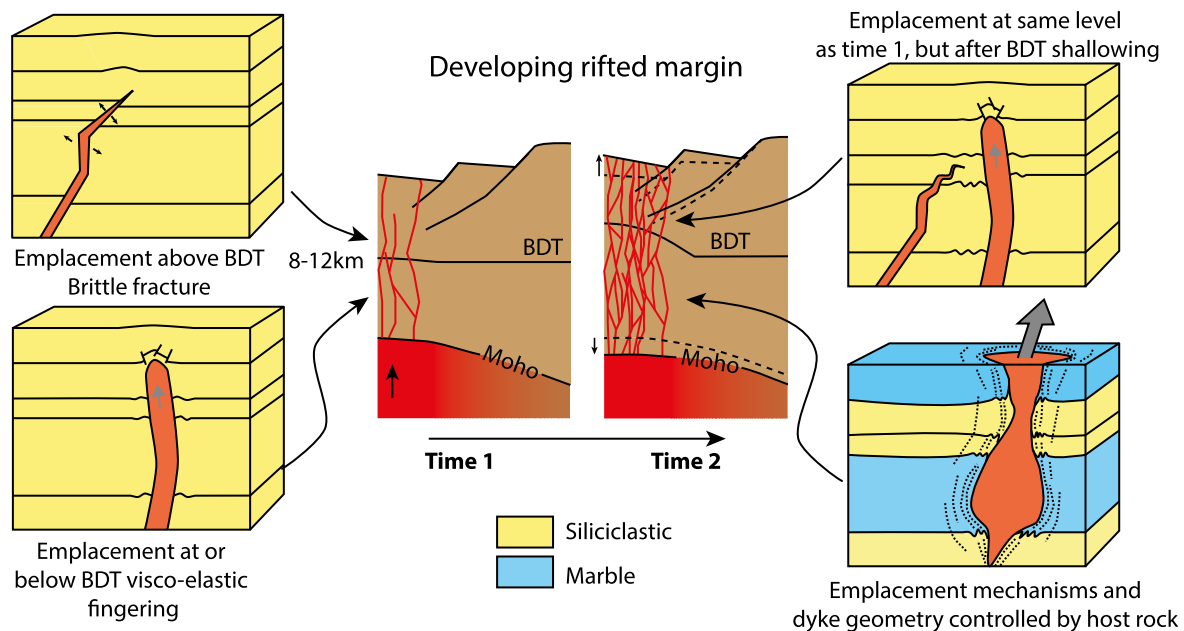
Fig. 10. Conceptual model showing evolution of the Brittle-Ductile Transition (BDT) during rifting and what type of dyke geometries can be expected at different levels in the rift. At Time 1, the BDT is slightly elevated due to rise of the underlying asthenosphere. Brittle fractures will govern the dyke emplacement above the BDT and visco-elastic fingering govern the emplacement at and below the BDT. This is also the case for Time 2, but the rise of the BDT causes ductile conditions where the dyke emplacement first was controlled by brittle mechanisms. Where the host rock is weak, like where carbonates dominate, the dyke morphology can become complex.

ment of the dyke swarm (Fig. 3 and Fig. 6). We propose that the fast emplacement and cooling of large volumes of mafic magma advected heat into the crust (e.g. Daniels et al., 2014; Kjøll et al., 2019), which lead to shallowing of the BDT, thinning of the brittle crust and a viscosity decrease of the ductile crust (Fig. 10). This process has the potential to considerably weaken the crust (Fig. 6D). Such an interpretation is in agreement with the model of Bastow and Keir (2011) which suggest that the intrusion of dykes in the East Africa Rift system and the Danakil depression induced weakening of the crust. Such mechanism can promote stretching and thereby thinning of the ductile crust and lithosphere, as well as brittle failure of the upper crust, leading to enhanced decompression melting and eventually the final break-up (Bastow et al., 2018; Keir et al., 2013). Our interpretation implies that fast, voluminous injection of magma can deeply and quickly modify the rheological structure of the lithosphere, which is proven to be a first-order parameter on tectonic deformation style (e.g. Clerc et al., 2015; Labrousse et al., 2016). However, models of continental rifting usually only account for the tectonic time-scale thermal evolution of the lithosphere, but not for the thermal impact of a short, voluminous magmatic event (e.g. Keller et al., 2013). Our study shows that implementing magma input is essential for revealing the tectonic evolution of magma-rich rifted margins.

5.3. Mechanical implications

A key observation from the studied outcrop is the two inclined dyke segment orientations. Several factors have been identified to control inclined dyke emplacement. First, the two dyke segment orientations are clearly contemporaneous and therefore conjugate, but with acute angles of about 30° rather than 60°, as would be expected under the Mohr-Coulomb brittle regime. Given that the dyke swarm was emplaced in a tectonic rift setting, the inclined dykes could be interpreted to be controlled by pre-existing conjugate extensional shear fractures. However, this hypothesis implies that we would expect an acute angle of ∼60° between the dyke orientations, in disagreement with the observed 30° acute angle. Second, topographic loading can deviate dyke trajectories

(Maccaferri et al., 2014). However, the deviation is expected to be gently gradual over the whole length of the dykes, which is incompatible with the observed abrupt orientation changes of the studied dykes (Fig. 3). Third, the interference between dykes intruding simultaneously can also lead to deviation of their trajectory (Kühn and Dahm, 2008). This mechanism, however, cannot explain the systematic grouping of the measured dyke orientations in two sets.

Other key observations necessary to explain the inclined conjugate orientations of the studied dykes are that (1) the opening of the dykes exhibit a shearing component (Fig. 3 and Fig. 4), and (2) the emplacement of the dyke swarm lead to crustal thickening (Fig. 5). These observations are in good agreement with the 2D experiments of Abdelmalak et al. (2012) and Bertelsen et al. (2018), which show that the forceful propagation of a dyke tip into a cohesive brittle crust is accommodated by a local conjugate set of small-scale shear structures that can control the subsequent oblique propagation of the tip. In these experiments, there were no tectonic extension. The resulting dykes consisted of steeply-dipping segments of alternating dip-directions. In addition, the emplacement of the dykes in these experiments also triggered surface uplift and thickening of the models. The similarity between these experiments and the observations presented here suggests that the oblique segments of the dykes are markers of a forceful dyke emplacement mechanism, i.e. the emplacing dykes generated their own stress field that overcame both the vertical load of the overburden and the tectonic stresses.

This mechanism is supported by seismological data, which show that the propagation of dykes in active volcanoes triggers significant shear failure of the host, where the fault planes exhibit small acute angle between groups of fault planes (Ágústsdóttir et al., 2016; White et al., 2011). Another mechanism has been proposed by Weinberg and Regenauer-Lieb (2010), who argue that conjugate micro-scale shear damage is triggered by ductile fracturing, which subsequently controls the orientation of the emplacing magma. These elements strongly suggest that hybrid mode I-II failure of the host rock plays a major role in the emplacement of the studied dyke swarm. This is in contradiction to the established

theory assuming pure mode I dyke propagation along a tensile fracture perpendicular to σ_3.

Our field observations show distinct modes of emplacement of the intrusions highlighted by contrasting deformation mechanisms of the host rock. Rubin (1993) and Galland et al. (2014) show that magma emplacement is controlled not only by the mechanical behaviour of the host rock, but also by the magma properties and emplacement rate. In our study area, all intrusions are of very similar mafic composition (Tegner et al., 2019) and have a similar magma crystallization temperature ($\sim$1150 °C) over the 900 km long exposure of the dyke complex (Kjøll et al., 2019). We infer that the magma properties along the whole dyke complex were relatively homogeneous, which strongly suggests that the observed emplacement mechanisms dominantly resulted from distinct brittle/ductile rheology of the host rock (Fig. 10).

The time scale of emplacement of mafic sheet intrusions (days to years) is orders of magnitude shorter than the rates of ductile tectonic deformation (10^{-13} to 10^{-15} s^{-1}; e.g. Sassier et al., 2009). This has been used to argue that at such short time scales, the ductile crust can rupture in a brittle fashion to accommodate the emplacement of dykes. However, our observations show that ductile deformation also plays a major role in accommodating the emplacement of magma in the study areas. This implies that the emplacement of dykes in the ductile crust is not necessarily controlled by brittle fracturing. This is corroborated by our field observations at Corrovarre and Sarek, which show that significant volumes of magma can be transported along sheets that are not purely brittle structures. The laboratory experiments of Bertelsen et al. (2018) show that sheet-like intrusions can form by viscoelastic fingering. In these experiments, the visco-elastic fingers exhibit straight, parallel walls and blunt tips that push their host rock ahead, exactly like the intrusions shown in Fig. 7. We infer that dykes in the ductile crust can be emplaced by viscoelastic fingering, so that their systematic interpretation as brittle structures should be done with caution. The observations presented here also imply that ductile deformation of the Earth's crust can take place at rates that are several orders of magnitude faster than tectonic strain rates.

6. Conclusions

This paper presents detailed field observations of a spectacularly exposed dyke swarm emplaced at 10 to 15 km depth at a magma-rich rifted margin related to the breakup of the palaeocontinents Baltica and Laurentia at $\sim$606 Ma. Such level of a magma-rich rifted margin is rarely exposed at the surface and these observations are relatively unique in this setting. This study, based on field examples from northern Sweden and Norway, allows us to reveal fundamental features related to (1) dyke emplacement mechanisms near the brittle-ductile transition, and (2) to discuss the geodynamic implications of the fast emplacement of a dyke swarm in a magma-rich rifted continental margin.

Our conclusions on dyke emplacement mechanisms are:

- The emplacement of numerous dykes was accommodated by brittle failure, whereas the emplacement of some dykes was accommodated by significant ductile deformation of the host rock.
- The brittle dykes form a conjugate set, separated by an average acute angle of 30° Hybrid mode I-II fracture propagation accommodated the emplacement of this conjugate dyke system, in disagreement with the commonly established models assuming a pure mode I propagation.
- The dyke-tip shapes and the associated brittle-ductile structures suggest that dykes can also be emplaced as 'visco-elastic fingers' near the brittle-ductile transition.

- In ductile host rock, magma conduits may exhibit strongly lobate shapes suggesting that magma transport can be accommodated dominantly by ductile flow of the host rock along finger-like channels.

The geodynamic implications of this study are the following:

- Dykes emplaced contemporaneously may exhibit two main orientations and demonstrate that dykes are not always systematically perpendicular to the rifting direction.
- The studied dyke swarm accommodated for both crustal stretching (94%) and crustal thickening ($\sim$27%), indicating that when magma emplacement rate is greater than tectonic stretching rate, the magma pressure can lift the overburden and thicken the crust.
- Even in an active rift setting, the dykes were emplaced in a forceful manner and did not accommodate passively for the tectonic stretching.
- The emplacement of the dyke swarm lead to a shallowing of the brittle-ductile transition.

Our study shows that the thermal impact of a dyke swarm can considerably weaken the crust and potentially affect the geodynamic evolutions of magma-rich rifted margins and be a major factor controlling continental break-up.

Acknowledgements

Appendix A. Supplementary material

Supplementary material related to this article can be found online at https://doi.org/10.1016/j.epsl.2019.04.016.

References

Abdelmalak, M.M., Andersen, T.B., Planke, S., Faleide, J.I., Corfu, F., Tegner, C., Shephard, G.E., Zastrozhnov, D., Myklebust, R., 2015. The ocean-continent transition in the mid-Norwegian margin: insight from seismic data and an onshore Caledonian field analogue. Geology 43 (11), 1011–1014.

Abdelmalak, M.M., Mourgues, R., Galland, O., Bureau, D., 2012. Fracture mode analysis and related surface deformation during dyke intrusion: results from 2D experimental modelling. Earth Planet. Sci. Lett. 359, 93–105.

Ágústsdóttir, T., Woods, J., Greenfield, T., Green, R.G., White, R.S., Winder, T., Brandsdóttir, B., Steinthórsson, S., Soosalu, H., 2016. Strike-slip faulting during the 2014 Bárðarbunga-Holuhraun dike intrusion, central Iceland. Geophys. Res. Lett. 43 (4), 1495–1503.

Allken, V., Huismans, R.S., Thieulot, C., 2012. Factors controlling the mode of rift interaction in brittle-ductile coupled systems: a 3D numerical study. Geochem. Geophys. Geosyst. 13, Q05010.

Anderson, E.M., 1905. The dynamics of faulting. Trans. Edinb. Geol. Soc. 8 (3), 387–402.

Anderson, E.M., 1936. The dynamics of the formation of cone sheets, ring dykes and cauldron subsidences. Proc. R. Soc. Edinb. 56, 128–163.

Andréasson, P.-G., Svenningsen, O., Johansson, I., Solyom, Z., Xiaodan, T., 1992. Mafic dyke swarms of the Baltica-Iapetus transition, Seve Nappe Complex of the Sarek Mts., Swedish Caledonides. GFF 114 (1), 31–45.

Andréasson, P.-G., Svenningsen, O.M., Albrecht, L., 1998. Dawn of Phanerozoic orogeny in the North Atlantic tract; evidence from the Seve-Kalak Superterrane, Scandinavian Caledonides. GFF 120 (2), 159–172.

Bastow, I.D., Booth, A.D., Corti, G., Keir, D., Magee, C., Jackson, C.A.L., Warren, J., Wilkinson, J., Lascialfari, M., 2018. The development of late-stage continental breakup: seismic reflection and Borehole evidence from the Danakil Depression, Ethiopia. Tectonics 37 (9), 2848–2862.

Bastow, I.D., Keir, D., 2011. The protracted development of the continent–ocean transition in Afar. Nat. Geosci. 4 (4), 248.

Bastow, I.D., Keir, D., Daly, E., 2011. The Ethiopia Afar Geoscientific Lithospheric Experiment (EAGLE): probing the transition from continental rifting to incipient seafloor spreading. Volcanism Evol. Afr. Lithosp. 478, 1–26.

Bertelsen, H.S., Rogers, B.D., Galland, O., Dumazer, G., Abbana Bennani, A., 2018. Laboratory modelling of coeval brittle and ductile deformation during magma emplacement into viscoelastic rocks. Front. Earth Sci. 6.

Buckley, S., Ringdal, K., Dolva, B., Naumann, N., Kurz, T., 2017. LIME: 3D visualisation and interpretation of virtual geoscience models. In: Proceedings EGU General Assembly Conference Abstracts, vol. 19, p. 15952.

Burchardt, S., Troll, V.R., Mathieu, L., Emeleus, H.C., Donaldson, C.H., 2013. Ardnamurchan 3D cone-sheet architecture explained by a single elongate magma chamber. Sci. Rep. 3.

Cawood, P.A., McCausland, P.J., Dunning, G.R., 2001. Opening Iapetus: constraints from the Laurentian margin in Newfoundland. Geol. Soc. Am. Bull. 113 (4), 443–453.

Clerc, C., Jolivet, L., Ringenbach, J.-C., 2015. Ductile extensional shear zones in the lower crust of a passive margin. Earth Planet. Sci. Lett. 431, 1–7.

Courtillot, V., Jaupart, C., Manighetti, I., Tapponnier, P., Besse, J., 1999. On causal links between flood basalts and continental breakup. Earth Planet. Sci. Lett. 166 (3), 177–195.

Daniels, K.A., Bastow, I., Keir, D., Sparks, R., Menand, T., 2014. Thermal models of dyke intrusion during development of continent–ocean transition. Earth Planet. Sci. Lett. 385, 145–153.

Galland, O., Burchardt, S., Hallot, E., Mourgues, R., Bulois, C., 2014. Dynamics of dikes versus cone sheets in volcanic systems. J. Geophys. Res., Solid Earth 119 (8), 6178–6192.

Halls, H.C., Fahrig, W.F., 1987. Mafic Dyke Swarms. Geological Association of Canada Special Paper, vol. 34. Toronto, Canada, 503 pp.

Jakob, J., Andersen, T.B., Kjøll, H.J., 2019. A review and reinterpretation of the architecture of the South and South-Central Scandinavian Caledonides—a magmapoor to magma-rich transition and the significance of the reactivation of rift inherited structures. Earth-Sci. Rev. 192, 513–528.

Kavanagh, J.L., 2018. Mechanisms of magma transport in the upper crust—dyking. In: Volcanic and Igneous Plumbing Systems, pp. 55–88.

Keir, D., Bastow, I.D., Pagli, C., Chambers, E.L., 2013. The development of extension and magmatism in the Red Sea rift of Afar. Tectonophysics 607, 98–114.

Keir, D., Pagli, C., Bastow, I.D., Ayele, A., 2011. The magma-assisted removal of Arabia in Afar: evidence from dike injection in the Ethiopian rift captured using InSAR and seismicity. Tectonics 30 (2).

Keller, T., May, D.A., Kaus, B.J., 2013. Numerical modelling of magma dynamics coupled to tectonic deformation of lithosphere and crust. Geophys. J. Int. 195 (3), 1406–1442.

Kjøll, H.J., Andersen, T.B., Corfu, F., Labrousse, L., Tegner, C., Abdelmalak, M.M., Planke, S., 2019. Timing of break-up and thermal evolution of a pre-Caledonian Neoproterozoic exhumed magma-rich rifted margin. Tectonics. https://doi.org/10.1029/2018TC005375.

Krumbholz, M., Hieronymus, C.F., Burchardt, S., Troll, V.R., Tanner, D.C., Friese, N., 2014. Weibull-distributed dyke thickness reflects probabilistic character of host-rock strength. Nat. Commun. 5, 3272.

Kühn, D., Dahm, T., 2008. Numerical modelling of dyke interaction and its influence on oceanic crust formation. Tectonophysics 447 (1–4), 53–65.

Labrousse, L., Huet, B., Le Pourhiet, L., Jolivet, L., Burov, E., 2016. Rheological implications of extensional detachments: Mediterranean and numerical insights. Earth-Sci. Rev. 161, 233–258.

Legrand, D., Calahorrano, A., Guillier, B., Rivera, L., Ruiz, M., Villagomez, D., Yepes, H., 2002. Stress tensor analysis of the 1998-1999 tectonic swarm of northern Quito related to the volcanic swarm of Guagua Pichincha volcano, Ecuador. Tectonophysics 344 (1–2), 15–36.

Lindahl, I., Stevens, B.P., Zwaan, K.B., 2005. The geology of the Vaddas area, Troms: a key to our understanding of the Upper Allochthon in the Caledonides of northern Norway. Nor. Geol. Unders. 445 (5).

Maccaferri, F., Rivalta, E., Keir, D., Acocella, V., 2014. Off-rift volcanism in rift zones determined by crustal unloading. Nat. Geosci. 7 (4), 297.

Magee, C., Muirhead, J.D., Karvelas, A., Holford, S.P., Jackson, C.A.L., Bastow, I.D., Schofield, N., Stevenson, C.T.E., McLean, C., McCarthy, W., Shtukert, O., 2016. Lateral magma flow in mafic sill complexes. Geosphere 12 (3), 809–841.

Menzies, M.A., Klemperer, S.L., Ebinger, C.J., Baker, J., 2002. Characteristics of volcanic rifted margins. In: Menzies, M.A., Klemperer, S.L., Ebinger, C.J., Baker, J. (Eds.), Volcanic Rifted Margins, vol. 362. Geological Society of America.

Mjelde, R., Digranes, P., Van Schaack, M., Shimamura, H., Shiobara, H., Kodaira, S., Naess, O., Sørenes, N., Vågnes, E., 2001. Crustal structure of the outer Vøring Plateau, offshore Norway, from ocean bottom seismic and gravity data. J. Geophys. Res., Solid Earth 106 (B4), 6769–6791.

Nakamura, K., 1977. Volcanoes as possible indicators of tectonic stress orientation—principle and proposal. J. Volcanol. Geotherm. Res. 2 (1), 1–16.

Pasquare, F., Tibaldi, A., 2007. Structure of a sheet-laccolith system revealing the interplay between tectonic and magma stresses at Stardalur Volcano, Iceland. J. Volcanol. Geotherm. Res. 161 (1–2), 131–150.

Pik, R., Marty, B., Carignan, J., Yirgu, G., Ayalew, T., 2008. Timing of East African Rift development in southern Ethiopia: implication for mantle plume activity and evolution of topography. Geology 36 (2), 167–170.

Rivalta, E., Taisne, B., Bunger, A.P., Katz, R.F., 2015. A review of mechanical models of dike propagation: schools of thought, results and future directions. Tectonophysics 638, 1–42.

Rubin, A.M., 1992. Dike-induced faulting and graben subsidence in volcanic rift zones. J. Geophys. Res., Solid Earth 97 (B2), 1839–1858.

Rubin, A.M., 1993. Dikes vs. diapirs in viscoelastic rock. Earth Planet. Sci. Lett. 119 (4), 641–659.

Saffman, P.G., Taylor, G., 1958. The penetration of a fluid into a porous medium or Hele-Shaw cell containing a more viscous liquid. Proc. R. Soc. Lond. Ser. A, Math. Phys. Sci. 245 (1242), 312–329.

Sassier, C., Leloup, P.-H., Rubatto, D., Galland, O., Yue, Y., Lin, D., 2009. Direct measurement of strain rates in ductile shear zones: a new method based on syntectonic dikes. J. Geophys. Res., Solid Earth 114 (B1).

Schofield, N., Alsop, I., Warren, J., Underhill, J.R., Lehné, R., Beer, W., Lukas, V., 2014. Mobilizing salt: magma-salt interactions. Geology 42 (7), 599–602.

Spacapan, J.B., Galland, O., Leanza, H.A., Planke, S., 2017. Igneous sill and finger emplacement mechanism in shale-dominated formations: a field study at Cuesta del Chihuido, Neuquén Basin, Argentina. J. Geol. Soc. 174 (3), 422–433.

Svenningsen, O.M., 1994a. The Baltica–Iapetus passive margin dyke complex in the Sarektjåkkå Nappe, northern Swedish Caledonides. Geol. J. 29 (4), 323–354.

Svenningsen, O.M., 1994b. Tectonic significance of the meta-evaporitic magnesite and scapolite deposits in the Seve Nappes, Sarek Mts., Swedish Caledonides. Tectonophysics 231 (1), 33–44.

Svenningsen, O.M., 1995. Extensional deformation along the Late Precambrian-Cambrian Baltoscandian passive margin: the Sarektjåkkå Nappe, Swedish Caledonides. Geol. Rundsch. 84 (3), 649–664.

Svenningsen, O.M., 2001. Onset of seafloor spreading in the Iapetus Ocean at 608 Ma: precise age of the Sarek Dyke Swarm, northern Swedish Caledonides. Precambrian Res. 110 (1), 241–254.

Svensen, H., Corfu, F., Polteau, S., Hammer, Ø., Planke, S., 2012. Rapid magma emplacement in the Karoo large igneous province. Earth Planet. Sci. Lett. 325, 1–9.

Tegner, C., Andersen, T.B., Kjøll, H.J., Brown, E.L., Hagen-Peter, G., Corfu, F., Planke, S., Torsvik, T., 2019. A mantle Plume origin for the Scandinavian Dyke Complex: a "piercing point" for the 615 Ma plate reconstruction of Baltica? Geochem. Geophys. Geosyst. 20, 1075–1094.

Weinberg, R.F., Regenauer-Lieb, K., 2010. Ductile fractures and magma migration from source. Geology 38 (4), 363–366.

White, R., McCausland, W.A., 2016. Volcano-tectonic earthquakes: a new tool for estimating intrusive volumes and forecasting eruptions. J. Volcanol. Geotherm. Res. 309, 139–155.

White, R.S., Drew, J., Martens, H.R., Key, J., Soosalu, H., Jakobsdóttir, S.S., 2011. Dynamics of dyke intrusion in the mid-crust of Iceland. Earth Planet. Sci. Lett. 304 (3–4), 300–312.

Zwaan, B.K., van Roermund, H.L., 1990. A rift-related mafic dyke swarm in the Corrovarre Nappe of the Caledonian Middle Allochthon, Troms, North Norway, and its tectonometamorphic evolution. Nor. Geol. Unders. Bull. 419, 25–44.